MASTER Optical Detection of the First LIGO/Virgo Neutron Star Binary Merger GW170817

V. M. Lipunov[1,2] , E. Gorbovskoy[2], V. G. Kornilov[1,2], N . Tyurina[2], P. Balanutsa[2], A. Kuznetsov[2], D. Vlasenko[1,2],
D. Kuvshinov[1,2], I. Gorbunov[2], D. A. H. Buckley[3], A. V. Krylov[2], R. Podesta[4], C. Lopez[4], F. Podesta[4], H. Levato[5], C. Saffe[5],
C. Mallamachi[6], S. Potter[3], N. M. Budnev[7], O. Gress[2,7], Yu. Ishmuhametova[7], V. Vladimirov[2], D. Zimnukhov[2], V. Yurkov[8],
Yu. Sergienko[8], A. Gabovich[8], R. Rebolo[9] , M. Serra-Ricart[9] , G. Israelyan[9], V. Chazov[2], Xiaofeng Wang[10] ,
A. Tlatov[11], and M. I. Panchenko[2]

[1] M.V.Lomonosov Moscow State University, Physics Department, Leninskie gory, GSP-1, Moscow, 119991, Russia; lipunov2007@gmail.com
[2] M.V.Lomonosov Moscow State University, Sternberg Astronomical Institute, Universitetsky pr., 13, Moscow, 119234, Russia
[3] South African Astrophysical Observatory, P.O. Box 9, 7935 Observatory, Cape Town, South Africa
[4] Observatorio Astronomico Felix Aguilar (OAFA), National University of San Juan, San Juan, Argentina
[5] Instituto de Ciencias Astronomicas, de la Tierra y del Espacio (ICATE), San Juan, Argentina
[6] National University of San Juan, San Juan, Argentina
[7] Irkutsk State University, Applied Physics Institute, 20, Gagarin Boulevard, Irkutsk, 664003, Russia
[8] Blagoveschensk State Pedagogical University, Lenin str., 104, Amur Region, Blagoveschensk, 675000, Russia
[9] Instituto de Astrofacuteisica de Canarias Via Lactea, s/n E-38205 La Laguna (Tenerife), Spain
[10] Tsinghua University, Haidian District, Beijing, 100084, China
[11] Kislovodsk Solar Station of the Main (Pulkovo) Observatory, RAS, P.O. Box 45, ul. Gagarina 100, Kislovodsk, 357700, Russia

Abstract

Following the discovery of the gravitational-wave source GW170817 by three Laser Interferometer Gravitational-wave Observatory (LIGO)/Virgo antennae (Abbott et al., 2017a), the MASTER Global Robotic Net telescopes obtained the first image of the NGC 4993 host galaxy. An optical transient, MASTER OTJ130948.10-232253.3/ SSS17a was later found, which appears to be a kilonova resulting from the merger of two neutron stars (NSs). Here we describe this independent detection and photometry of the kilonova made in white light, and in B, V, and R filters. We note that the luminosity of this kilonova in NGC 4993 is very close to those measured for other kilonovae possibly associated with gamma-ray burst (GRB) 130603 and GRB 080503.

Key words: binaries: general – gravitational waves – methods: observational – stars: neutron

Supporting material: animation

1. Introduction

There are several reasons to assume that neutron-star (NS) mergers must be accompanied by electromagnetic radiation before, during, and after the gravitational-wave pulse. Blinnikov et al. (1984) were the first to associate gamma-ray bursts with the explosion of an NS during a merger.

Lipunov & Panchenko (1996) showed that a merger of two magnetized NSs (or one such star if the second component is a black hole) can be expected to be accompanied by a non-thermal electromagnetic burst, the precursor of a pulsar. Later, Hansen et al. (2001) illustrated the theory of Lipunov & Panchenko (1996) using a detailed electromagnetic model.

After a merger (Clark et al. 1979), some of the matter from the NS can be ejected and this may result in the radioactive decay of the synthesized heavy elements—a so-called kilonova (Li & Paczynski 1998; Metzger et al. 2010; Berger et al. 2013; Tanvir et al. 2013). On the other hand, a rapidly rotating self-gravitating object—a spinar—may be a source of strong, long bursts of electromagnetic radiation (Lipunova & Lipunov 1998; Lipunov & Gorbovskoy 2008; Lipunova et al. 2009). The spinar may represent an intermediate phase, and its rotational evolution may end up in the formation of a highly magnetized heavy NS, called a magnetar.

The MASTER Global Robotic Net has been taking an active part in the follow-up searches for optical afterglows of all detected LVC events (Lipunov et al. 2017a, 2017b) since the detection of the first gravitational-wave event with the advanced Laser Interferometer Gravitational-wave Observatory (LIGO) interferometers (Abbott et al. 2016a, 2016b).

On 2017 August 17, von Kienlin et al. (2017) reported a short (2 s long) gamma-ray burst recorded by the Gamma-ray Burst Monitor (GBM) mounted on the *Fermi* satellite (*Fermi* GBM trigger 524666471) at 12:41:06.47 UT, which occurred 2 s after the detection of the gravitational-wave event (Connaughton et al. 2017; LIGO Scientific Collaboration & Virgo Collaboration 2017a). Later, Savchenko et al. (2017) also found a short and relatively weak transient with an $S/N > 3$, coincident with the GBM trigger (Abbott et al. 2017b).

On the following day, the 1 m SWOPE telescope at Las Campanas Observatory was the first to report the new optical source, SSS17a, located 5.3 arcsec E and 8.8 arcsec N of an S0 galaxy in the NGC 4993/ESO 508-G018 group, at a distance of ~40 Mpc (Cook et al. 2017; Coulter et al. 2017), also independently discovered by the MASTER auto-detection system (Lipunov et al. 2017a), and confirmed by other telescopes in different filters in the first hours (Abbott et al. 2017a, 2017b). Electromagntic (EM) partners also started their broadband investigations (Abbott et al. 2017a, 2017b; Chambers et al. 2017; Drout et al. 2017; Shara et al. 2017).

MASTER Global Robotic Net observations of the G298040/ GW170817 error region started with the MASTER-SAAO, in South Africa, on 2017 August 17 17:06:47 UT (0.4 days after trigger), then continued in MASTER-IAC, in Spain, on 2017 August 17 20:29:26 UT, and in Argentina with the

Figure 1. MASTER Global Robotic Net and LVC interaction in GW170817.

MASTER-OAFA, which obtained the first image of NGC 4993 at 22:54:18 UT using the very wide field cameras; however, it did not detect any optical transient, to a limit of $m = 15.2$ (5σ in white light and corrected for Galaxy extinction). In other words, MASTER-OAFA obtained the first image of the NGC 4993 galaxy after the NS–NS merger.

The optical transient MASTER OTJ130948.10-232253.3/SSS17a was independently discovered by the MASTER-OAFA auto-detection system during inspection by the main MASTER-OAFA telescope at 23:59:54 UT (Abbott et al. 2017a, 2017b; Lipunov et al. 2017a, 2017b, 2017c, 2017d).

These discoveries and subsequent observations showed quite conclusively that on 2017 August 17 astronomers observed a merger of two NSs in the galaxy NGC 4993 and its afterglow, and that this was the first time such an event was observed, not only in gravitational waves, but also over the electromagnetic spectrum including gamma-rays, X-rays, ultraviolet, optical, and infrared radiation. This first detection of an electromagnetic counterpart comes only two years after the first confirmed detection of a gravitational-wave event. This is in comparison to the three decades in took for the equivalent detection of gamma-ray bursts at other wavelengths.

2. MASTER Global Robotic Net in LIGO/Virgo Follow-up

The MASTER Global Robotic Net (Lipunov et al. 2010) consists of two classes of instruments: the main MASTER system of twin 40 cm wide field ($2 \times 4\,\mathrm{deg}^2$, 1 pixel = 1.9 arcsec) optical robotic telescopes, and two very wide field cameras (MASTER-VWF). MASTER-VWF is a very fast camera capable of obtaining up to three images per second and equipped with an 82 mm aperture F/1.2 lens giving a $16 \times 24° = 384\,\mathrm{deg}^2$ field of view (FOV), capable of detecting objects down to a limiting

magnitude of 12^m per single 5 s exposure image. Each of the MASTER-Net observatories are equipped with two MASTER-VWF cameras, which are fixed on the same mount as the main MASTER-II telescopes; together they cover a $32 \times 24°$ area centered on the main MASTER telescope direction. For more details see Lipunov et al. (2010), Kornilov et al. (2012), and Gorbvskoy et al. (2010, 2013).

MASTER nodes are located at the following observatories: MASTER-Amur, MASTER-Tunka, MASTER-Kislovodsk, MASTER-Tavrida, MASTER-Ural (Russia), MASTER-SAAO (South Africa), MASTER-IAC (Teyde Observatory, Canarias, Spain), and MASTER-OAFA (San Juan National University Observatory, Argentina; see Figure 1).

All MASTER observatories are equipped with their own identical photometers (two full-frame CCD cameras; B, V, R, I Johnson-Bessel filters; and two linear polarizers) and are controlled by identical software. The use of identical equipment allows us to have up to 24-hour continuous observations of optical counterparts of transients in identical photometric systems. Hence, combining photometric data for different transients observed from different parts of the MASTER Global Robotic Net is a proven astronomical process (see the latest results in Lipunov et al. 2016; Troja et al. 2017a).

The large FOV of every MASTER main telescope allows us to use a large number (1000–5000) of reference stars for photometric reductions. As a result, photometric errors can be minimized using large catalogs such as Tycho II and USNO-B1.

We have had successful experiences in the advanced LIGO follow-up campaign during the investigation of GW150914 (Abbott et al. 2016a, 2016b; Lipunov et al. 2017e, 2017f), as MASTER provided the most input to the optical support of this event (see Table 1 and Section 5 in Abbott et al. 2016c).

3. GW170817 MASTER Observations

The first alert of the LIGO/Virgo G298048 event arrived when it was daytime at most of the MASTER Global Robotic Net observatories. It was nighttime at MASTER-Amur, in the Russian Far East, but observations were prevented by unfavorable weather conditions.

MASTER Global Robotic Net started observing the LIGO/Virgo G298048 error field on 2017 August 17 17:06:47 UT (Lipunov et al. 2017a, 2017b, 2017c, 2017d).

MASTER-SAAO automatically began to observe part of the common area of the initial LIGO BAYESTAR error region received by the socket connection (LIGO Scientific Collaboration & Virgo Collaboration 2017a) and the *Fermi* GBM error box (Connaughton et al. 2017) immediately after sunset (Sun altitude $<12°$) on 2017 August 17 17:06:47 UT = 2017 August 17.71304 (JD = 2457983.21304398); i.e., 15,943 s after the LIGO/Virgo Collaboration (LVC) trigger time (12:41:04 UT), MASTER-IAC began the GW170817 initial BAYESTAR map inspection, on 2017 August 17 20:29:26 UT (see Figure 1).

The first co-added unfiltered images (3×180 s images) have a limiting magnitude of $19^{m}.8$. This first stacked image also covered the most probable IceCube candidate N4 (Bartos et al. 2017). However, no optical transients were found in this error region.

The MASTER-SAAO telescopes then continued to observe the initial *Fermi* and LVC common error area and all IceCube candidates. The unfiltered limiting magnitudes and fields can be found in GraceDB, and the coverage map is available in Figure 2. No optical transients were found during these observations.

The localization map of LIGO/Virgo G298048 (LIGO Scientific Collaboration & Virgo Collaboration 2017c) was received at a time when the entire new small error field (it was small compared to the previous one, but still spanned a 125 deg^2 area; 3σ, i.e., 99.7% region area) was below the horizon for both MASTER-SAAO in South Africa and MASTER-IAC in the Canary Islands. The error field was above the horizon only for the MASTER-OAFA telescope in Argentina, but it was still daytime when the message was received.

The MASTER-OAFA, located at Observatorio Astronomico Felix Aguilar (OAFA, National University of San Juan, Argentina), also with two MASTER-VWF cameras, began imaging the new BAYESTAR-HLV (Singer & Price 2016; Singer et al. 2016) localization map of LIGO/Virgo G298048 (LIGO Scientific Collaboration & Virgo Collaboration 2017a, 2017b, 2017c) on 2017 August 17 22:54:18 UT, immediately after sunset. Observations started for the first field at R.A., decl. = $12^{h}59^{m}00^{s}.00-19^{d}59^{m}38^{s}.00$.

The main MASTER telescope imaged BAYESTAR-HLV localization map did not, unfortunately, cover the NGC 4993 region. But MASTER-OAFA VFW cameras (with a larger FOV) obtained the first image of the NGC 4993 galaxy after the NS–NS merger (Lipunov et al. 2017a, 2017d).

4. MASTER OTJ130948.10-232253.3/SSS17a in NGC 4993 Observations

There are two MASTER very wide field cameras (combined FOV = 760 deg^2, 22 arcsec pixel^{-1}) on the same MASTER-OAFA mount. As a result, we have a large series (a "video") of 5 s MASTER-VWF camera images taken without time gaps and covering the entire LIGO/Virgo *BAYESTAR-HLV* G298048 error box including the NGC 4993 galaxy (Figure 2(a)).

The MASTER-VWF cameras produce a huge data flow of 200 Gb day^{-1}, making it impossible for us to store all single-image frames for a long time. All single (5 s) VWF camera images obtained during main MASTER instrument exposures (typically 180 s) and CCD readouts ($\sim$30 s) are automatically co-added and archived.

The MASTER-OAFA telescope conducted an inspection survey of the LIGO/Virgo G298048 field quite close ($<10°$) to the NGC 4993 position, and therefore this position is covered by almost all co-added VWF camera images obtained during this survey. In order to obtain the deepest early observation of NGC 4993, we additionally stacked the first six co-added sets of images, taking into account the fact that the region happens to be on different parts of the frames. We thus obtain an extra stacked co-added image of NGC 4993, comprising 225 five-second single-exposures by MASTER-VWF images with mlim $\sim$15.5 mag l (Figure 2(b)).

The galaxy NGC 4993 can be seen in these co-added images, beginning from 2017 August 17 22:54:18 UT. For our analysis we also used an archival reference image obtained during the previous nights, with the same limiting magnitude. With the reference image subtracted, the very wide field camera images do not show the optical counterpart (see Table 1 and Figure 2(b)) at the NGC 4993 position, down to the V-band limiting magnitude of 15.5 mag.

As the LIGO/Virgo G298048 BAYESTAR-HLV (LIGO Scientific Collaboration & Virgo Collaboration 2017a, 2017b, 2017c) error region was rapidly setting, MASTER-OAFA only had a $\sim$3.5 hr window to observe the error field. Starting from 2017 August 17 22:58:48 UT, MASTER-OAFA observed the new BAYESTAR-HLV localization map of LIGO/Virgo G298048 with unfiltered images (180 s exposures), down to a limiting magnitude of 19–20^{m}. The co-added images (n frames added) have a fainter limiting magnitude of 20.5.

The final BAYESTAR-HLV localization map is highly elongated, and therefore fields with different priorities set at different times. A special program, *MASTER-Net scheduler*, distributed the sequence of survey images in such a way as to maximize the probable total observing time of the area inside the localization region before it set. In this particular case, the MASTER-OAFA telescope was the only MASTER telescope observing the localization region, but the *MASTER-Net scheduler* is designed to ensure the fastest possible coverage of the gravitational-wave (GW) error area by the MASTER telescope network. Figures 2(c) and (d) show the dynamics of the inspection survey and the coverage map on the first night since the beginning of observation until the last possible field inside BAYESTAR-HLV localization map disappears beyond the horizon.

During the survey of the GW error region, the MASTER-OAFA robotic telescope took two images of the galaxy NGC 4993 and our auto-detection system discovered MASTER OTJ130948.10-232253.3, also discovered by the SWOPE telescope and called SSS17a (later also named AT 2017gfo). It was first published in Coulter et al. (2017) and confirmed by multi-wavelength observations (see Abbott et al. 2017b). MASTER images were taken approximately 1 hr after the start of the survey, on 2017 August 17 23:59:54 UT, i.e., $11^{h}18^{m}50^{s}$ after the LVC trigger time (Lipunov et al. 2017a, 2017c, 2017d).
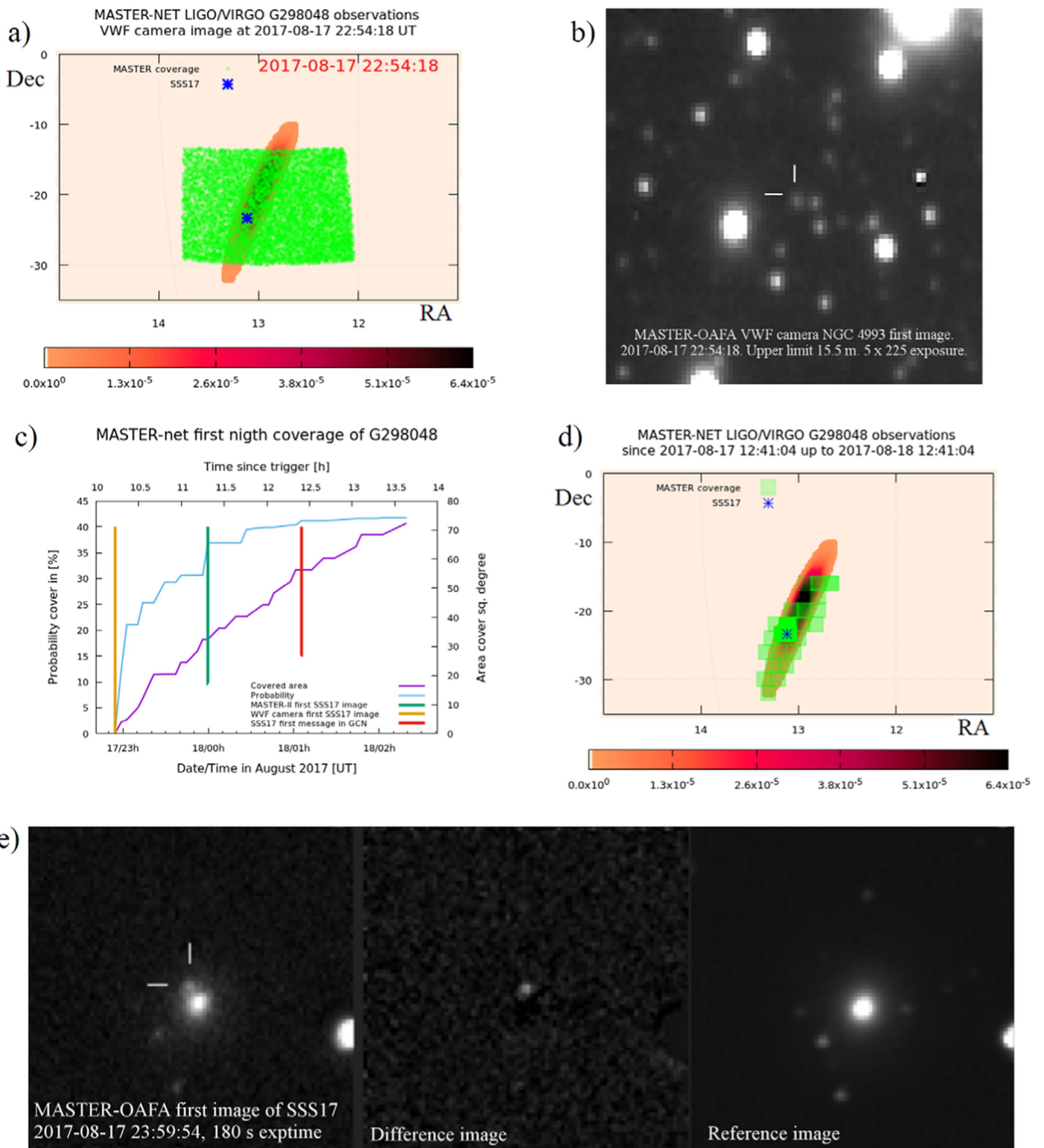
Figure 2. (a) MASTER-OAFA very wide field camera (VWFC) coverage of GW170817 error field starting from 2017 August 17 22:58:48 UT = 2017 August 17 22:54:18 UT. The color scale demonstrates G298048 probability distribution. (b) The first image of the NGC 4993 galaxy, 10 hr after the LVC GW170817/G298048 trigger. The image was taken with the MASTER VWFC (Lipunov et al. 2010) on the MASTER-OAFA telescope (Argentina). (c) The dynamics of MASTER Global Robotic Net LIGO/Virgo G298048 BAYESTAR-HLV error area inspections during the first night after the GW170817 (G298048) trigger. The blue line shows the growth of the coverage of the NGC 4993 galaxy where possible Kilonova MASTER OTJ130948.10-232253.3/SSS17a was automatically observed by MASTER-VWF cameras and the MASTER-OAFA telescope 2.5 and ~1.5 hr, respectively, before the SWOPE telegram (Coulter et al. 2017). (d) MASTER Global Robotic Net inspection of LIGO/Virgo G298048 BAYESTAR-HLV error area. The first-night coverage map by MASTER telescopes with the limiting magnitude of 20.5. (e) The first MASTER-OAFA image of the kilonova MASTER OTJ130948.10-232253.3/SSS17a in the galaxy NGC 4993, taken starting from 2017 August 17 23:59:54 UT (exposure = 180 s), 40.73 ks after the LVC GW170817/G298048 trigger time. The left panel shows the image obtained after subtracting 75% of the reference image.

(An animation of this figure is available.)

Table 1
MASTER Photometry of MASTER OTJ130948.10-232253.3/SSS17a (Galaxy Extinction Corrected; Schlafly & Finkbeiner 2011)

| Date	UT Start	Tstart–Ttrig, ks	Tmid–Ttrig, ks	Exp, s	Filter	Mag.	Err. Mag.	Upper Limit	MASTER Site
2017 Aug 17	22:54:18	36.794	37.356	225 × 5	V	>15.2	⋯	15.5	MASTER-OAFA-VWFC
2017 Aug 17	23:59:54	40.730	40.820	180	W	17.5	0.2	19.5	MASTER-OAFA
2017 Aug 18	00:19:05	41.881	41.971	180	W	17.1	0.2	19.3	MASTER-OAFA
2017 Aug 18	17:06:55	102.352	102.653	6 × 180	W	17.3	0.2	20.0	MASTER-SAAO
2017 Aug 18	17:17:33	102.989	103.463	3 × 180	R	17.0	0.2	19.8	MASTER-SAAO
2017 Aug 18	17:34:02	103.979	104.290	3 × 180	B	18.1	0.1	19.5	MASTER-SAAO
2017 Aug 19	17:06:57	188.753	189.047	3 × 180	W	18.4	0.2	20.0	MASTER-SAAO
2017 Aug 19	17:53:34	191.550	191.844	3 × 180	R	18.0	0.3	19.8	MASTER-SAAO
2017 Aug 19	18:04:32	192.208	192.503	3 × 180	B		⋯	19.5	MASTER-SAAO
2017 Aug 19	23:13:20	210.736	211.785	10 × 180	W	18.8	0.2	20.7	MASTER-OAFA
2017 Aug 20	17:04:36	275.012	275.306	3 × 180	W	>19.1	⋯	20.0	MASTER-SAAO
2017 Aug 20	17:25:56	276.292	276.586	3 × 180	R	>18.6	⋯	19.5	MASTER-SAAO
2017 Aug 20	17:36:32	276.928	277.222	3 × 180	B	>19.3	⋯	20.0	MASTER-SAAO
2017 Aug 21	00:26:31	301.527	302.577	10 × 180	W	>19.8	⋯	20.7	MASTER-OAFA
2017 Aug 21	17:08:14	361.630	361.925	3 × 180	W	>19.1	⋯	20.0	MASTER-SAAO
2017 Aug 21	18:06:12	365.108	365.403	3 × 180	R	>18.6	⋯	19.5	MASTER-SAAO
2017 Aug 21	19:20:23	369.559	369.854	3 × 180	B	>18.3	⋯	19.0	MASTER-SAAO

Note. Photometry was made on MASTER VWFC and on the main MASTER telescope (as can be seen from the limit value). This is the photometry of the faint stellar image derived from image subtraction, removing the galaxy contribution. Ttrig—LVC trigger Time. Tstart—MASTER exposure start time. Tmid—MASTER exposure middle time. $W = 0.8R + 0.2B$—unfiltered with respect to USNO-B1 stars. VWFC—Very Wide Field Camera, MASTER-SAAO and MASTER-OAFA—main MASTER telescopes at these observatories.

As is evident from Figure 2(e), the optical transient (OT) is visible in the subtracted image. The MASTER network software is constantly being improved and for some types of objects, for which it is possible to define several unquestionable automatic verification criteria, the discoveries are published automatically. Examples include gamma-ray bursts (GRBs) registered by the *Swift* satellite or near-Earth object (NEO) asteroid hazards. For example, the optical counterpart for GRB 161017A was observed, detected, and a discovery notice automatically published on the Gamma-ray Coordinates Network (GCN) approximately 200 s after the notice time (see Yurkov et al. 2016).

However, other types of objects require manual checks before publishing. G298048 was observed in the middle of the night in Moscow, and we only detected this OT by inspecting software reports in the morning of 18 August, i.e., several hours after another team had reported it (Abbott et al. 2017b; Coulter et al. 2017).

Once the optical source was found, the MASTER Global Robotic Net telescopes stopped the inspection survey inside the LIGO/Virgo probability map, and focused on observing MASTER OTJ130948.10-232253.3/SSS17a (Figures 2(b), (d), (e)).

For us, the most important factor in the argument that this OT in NGC 4993 is connected with GW170817 is its unusual spectral properties (Abbott et al. 2017b; Chen et al. 2017; Shara et al. 2017). The MASTER network has detected about ~1500 OTs in last several years, covering 10 different classes of astrophysical types: GRB optical counterparts (MASTER is the world leader in prompt optical GRB observations), supernovae, novae, dwarf novae, other cataclysmic variable, AGN and quasi-stellar object (QSO) flares, as well as anti-transients (dramatically decreased brightness of the stars), comets, potentially hazardous asteroids, ~15-minute-duration UVCet flares, and very short OTs of unknown nature (in two tubes simultaneously). The OT in NGC 4993 was really unlike any of our previously discovered transients. We decided that the appearance of this unusual object, in the LIGO/VIRGO error box 0.5 days after GW event, was not random and we focused on the photometry of this unusual object over subsequent nights.
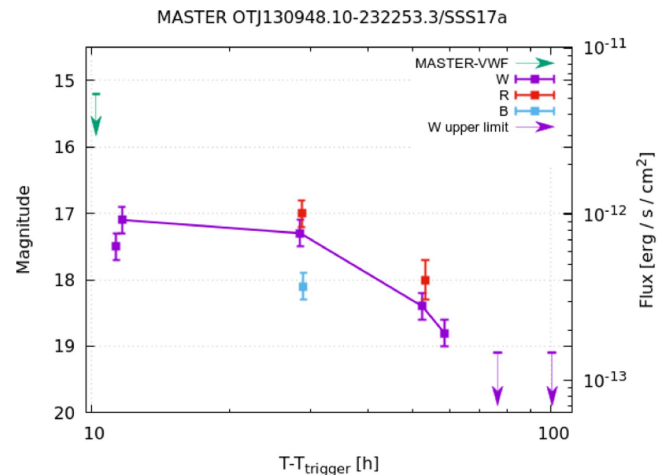
Figure 3. MASTER Global Robotic Net light curve of kilonova GW170817 in NGC 4993 (see Table 1).

Over the next three days both of the southern MASTER robotic telescopes, MASTER-SAAO and MASTER-OAFA, monitored the possible kilonova (Lipunov 2017), which remained visible for the two instruments in the B- and R-band filters and in unfiltered mode. Table 1 presents the results of the photometry that was made on subtracted images free from the galaxy background.

As of 2017 September 1, MASTER-OAFA and MASTER-SAAO had made a total of more than 600 exposures of the MASTER OTJ130948.10-232253.3/SSS17a region.

MASTER OTJ130948.10-232253.3/SSS17a photometry is listed in Table 1 and Figure 3 and is described in the following section.

5. Photometry

The usual MASTER auto-detection software identifies new or known objects automatically and undertakes photometry using calibrations provided by thousands of USNO-B1 stars in
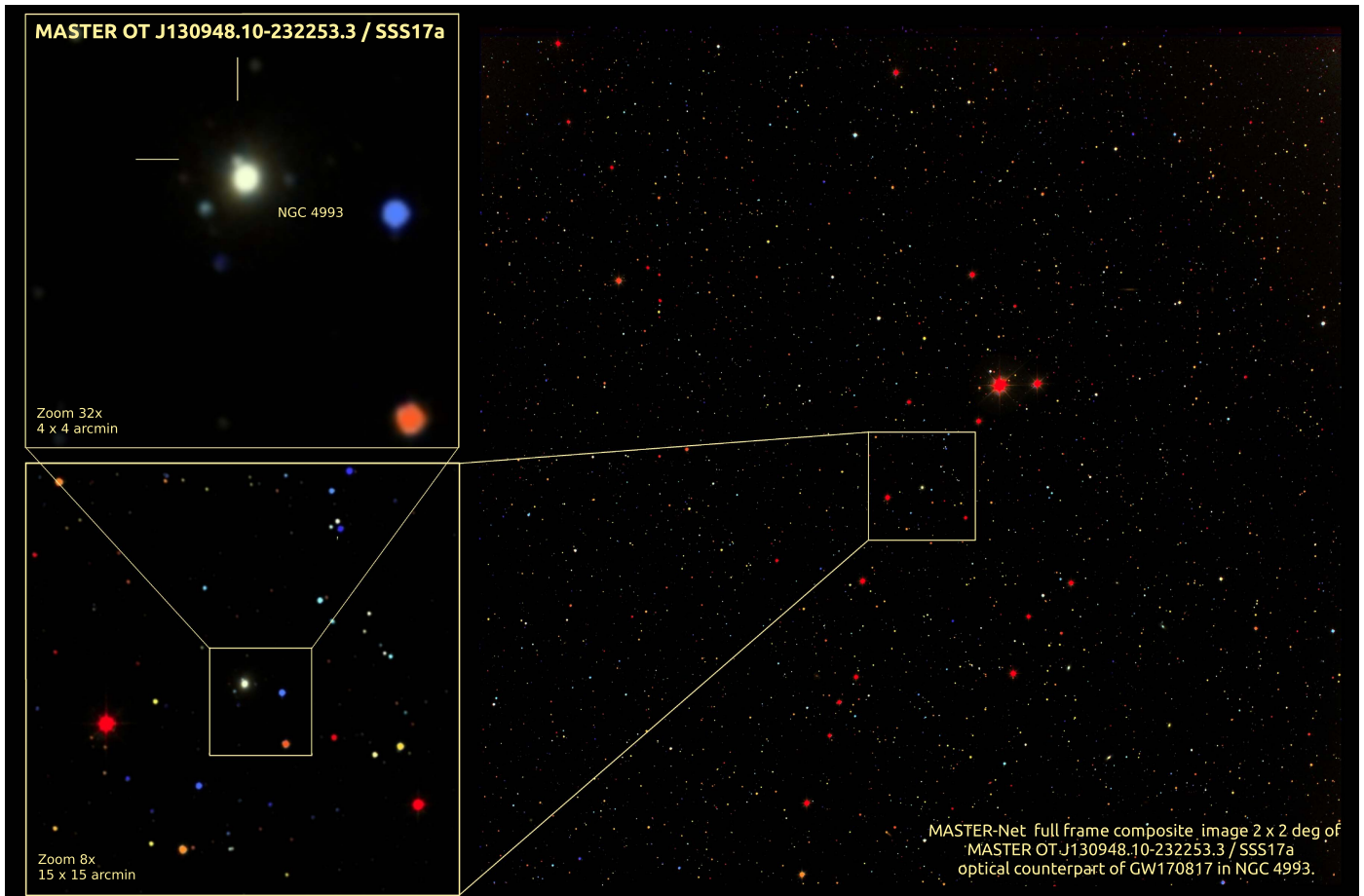
Figure 4. MASTER-composed discovery image started 2017 August 17 at 23:59:54 UT. We used color B, R, I, W filters, MASTER-OAFA, and MASTER-SAAO images. The kilonova position is marked by white lines on the left part of composed image. The right (large) image is the MASTER main telescope's usual FOV.

Table 2
Possible Kilonova Brightness

Name	Z	DL Mpc	DM	Obs.	Band	m_{vis} Max[AB]	MabsFlat spec AB	Flux iso erg s^{-1}	Link
Kilonova NGC 4993	0.0098	42.5	33.14	MASTER	W	17.3	−16.03	10^{42}	This paper
GRB 130603	0.3560	1911.9	41.41	*HST*	H	25.73	−15.35	5.50×10^{41}	Tanvir et al. (2013)
GRB 080503	0.561[*]	3290.5	42.59	Gemini/Keck	r	25.48	−16.62	1.78×10^{42}	Perley et al. (2009)

our wide FOV (Lipunov et al. 2010), in real time (1–2 minutes after a charge-coupled device (CCD) readout), and can work in alert, inspect, and survey mode, independently of human intervention. This is a unique feature that gives us the ability to detect new objects in large fields in real time and to study outbursts in the early stages of explosion (Lipunov et al. 2016; Troja et al. 2017).

It is impossible to produce photometry of this object using standard aperture or point-spread function (PSF) photometry methods on the original image due to the galaxy background. For accurate photometry we undertake the following procedure. For the subtraction procedure, we choose the most suitable reference image (by the average star FWHMs and the frame detection limit) from our archive. After a very accurate (sub-pixel) centering of the source and reference images, we obtain a difference image following the technique described in Alard (2000). Using the original image, we determine the transformation of the instrumental flux into standard stellar magnitudes, and then we measure

the object's instrumental flux from the difference image. We correct the obtained stellar magnitudes for the Galactic extinction, based on $E(B - V) = 0.1$ mag (Schlafly & Finkbeiner 2011).

The MASTER Global Robotic Net archive contains 126 images of the galaxy NGC 4993, obtained from 2015 January 17 00:45:46 to 2017 May 02 22:17:04, none of which show any optical activity for SSS17a (see Table 3).

In Figure 4 we present the MASTER-composed discovery image with kilonova position.

6. Discussion

The detection of EM radiation accompanying the coalescence of NSs was by no means a surprise. The merger of NSs as a formation mechanism of GRBs was first considered by Blinnikov et al. (1984), and the occurrence rate of such events was computed in 1987 using the population synthesis method ("Scenario Machine") by Lipunov et al. (1987) and later refined by taking

Table 3
MASTER Global Robotic Net's 126 Prediscovery Images of G298048's
Optical Counterpart from 2015 January 17 00:45:46
until 2017 May 02 22:17:04 UT

Date, UT	Exp.time, s	Filter	Upper_limit
2017 May 02 22:17:04.118	60	W	19.73
2017 May 02 22:03:32.383	60	W	19.70
2017 Apr 19 00:05:48.714	60	W	19.43
2017 Apr 18 23:54:57.474	60	W	19.49
2017 Mar 10 22:39:05.35	60	W	18.79
2017 Mar 10 22:39:05.349	60	W	18.70
2017 Mar 10 22:26:22.364	60	W	18.80
2017 Mar 10 22:26:22.343	60	W	18.70
2017 Mar 10 22:15:13.272	60	W	18.73
2017 Mar 10 22:15:13.25	60	W	18.70
2017 Feb 08 01:25:35.584	60	W	19.50
2017 Feb 08 01:14:42.231	60	W	19.50
2016 Dec 16 02:36:26.611	60	W	16.92
2016 Dec 16 02:36:26.59	60	W	17.00
2016 Dec 16 02:04:04.222	60	W	17.94
2016 Dec 16 02:04:04.21	60	W	17.90
2016 Aug 28 17:34:48.436	60	W	18.93
2016 Aug 28 17:33:09.212	60	W	19.04
2016 Aug 28 17:27:45.208	60	W	19.10
2016 Aug 28 17:27:45.208	180	W	19.64
2016 Aug 28 17:26:01.303	60	W	19.06
2016 Aug 28 17:20:34.987	60	W	18.65
2016 Aug 28 17:18:57.252	180	W	19.44
2016 Aug 28 17:18:57.252	60	W	18.60
2016 Aug 20 18:01:44.034	60	W	19.40
2016 Aug 20 17:56:18.846	60	W	19.42
2016 Aug 20 17:50:54.677	60	W	19.32
2016 Jun 21 18:53:44.099	60	W	19.21
2016 Jun 21 18:53:44.096	60	W	19.10
2016 Jun 21 18:43:23.665	60	W	19.14
2016 Jun 21 18:43:23.626	60	W	19.21
2016 Jun 21 18:32:58.607	60	W	19.21
2016 Jun 21 18:32:58.605	60	W	19.10
2016 Jun 17 21:53:12.354	60	W	18.56
2016 Jun 17 21:42:16.583	60	W	18.51
2016 Jun 17 21:31:33.343	60	W	18.50
2016 May 11 19:16:34.03	60	W	19.74
2016 May 1119:16:34.003	60	W	19.67
2016 May 11 19:03:15.997	60	W	19.77
2016 May 11 19:03:15.994	60	W	19.65
2016 May 11 18:51:12.122	60	W	19.73
2016 May 11 18:51:12.097	60	W	19.70
2016 May 05 20:20:07.211	180	W	20.00
2016 May 05 20:16:37.894	180	W	20.05
2016 May 05 20:13:09.175	180	W	20.00
2016 May 05 19:47:44.764	180	W	20.16
2016 May 05 19:44:10.718	180	W	20.13
2016 May 05 19:40:37.21	180	W	20.16
2016 May 05 19:14:58.806	180	W	20.53
2016 Apr 12 01:36:46.999	180	W	19.75
2016 Apr 12 01:36:46.996	180	W	19.58
2016 Apr 12 01:32:18.804	180	W	19.86
2016 Apr 12 01:32:18.799	180	W	19.60
2016 Apr 12 01:17:06.783	180	W	19.70
2016 Apr 12 01:17:06.781	180	W	19.67
2016 Apr 12 01:17:06.781	540	W	19.92
2016 Apr 12 00:59:15.746	180	W	20.06
2016 Apr 12 00:59:15.743	180	W	20.10
2016 Feb 21 00:29:56.411	60	W	19.21
2016 Feb 21 00:19:43.054	60	W	19.36
2016 Feb 21 00:09:02.759	60	W	19.39
2015 Dec 15 01:37:02.481	60	W	19.40

Table 3
(Continued)

Date, UT	Exp.time, s	Filter	Upper_limit
2015 Dec 15 01:37:02.477	60	W	19.15
2015 Dec 15 01:30:20.686	60	W	19.36
2015 Dec 15 01:30:20.684	60	W	19.09
2015 Dec 15 01:25:16.74	60	W	19.30
2015 Dec 15 01:25:16.729	60	W	19.07
2015 Nov 29 02:32:56.228	60	W	15.74
2015 Nov 29 02:32:56.197	60	W	15.60
2015 Nov 29 02:29:35.963	60	W	16.27
2015 Nov 29 02:29:35.937	60	W	15.91
2015 Nov 29 02:28:00.948	60	W	16.03
2015 Nov 29 02:28:00.93	60	W	16.42
2015 Nov 29 02:26:25.431	60	W	16.55
2015 Nov 29 02:26:25.431	180	W	17.17
2015 Nov 29 02:26:25.428	180	W	16.74
2015 Nov 29 02:26:25.428	60	W	16.16
2015 Aug 29 17:44:19.853	60	W	17.39
2015 Aug 29 17:37:59.363	60	W	17.45
2015 Aug 29 17:31:31.398	60	W	17.65
2015 Aug 29 17:29:59.822	60	W	17.76
2015 Aug 29 17:29:59.822	180	W	18.39
2015 Jun 30 20:25:08.182	60	W	18.75
2015 Jun 30 20:25:08.178	60	W	18.48
2015 Jun 30 20:13:55.063	60	W	18.84
2015 Jun 30 20:13:55.02	60	W	18.61
2015 Jun 30 20:02:44.457	60	W	17.80
2015 Jun 30 20:02:44.434	60	W	18.05
2015 Jun 20 18:15:48.359	60	W	19.94
2015 Jun 20 18:04:13.291	60	W	19.91
2015 Jun 20 17:52:43.813	60	W	19.80
2015 Apr 24 20:29:52.994	60	W	19.73
2015 Apr 24 20:29:52.966	60	W	19.56
2015 Apr 24 20:23:26.48	60	W	19.56
2015 Apr 24 20:23:26.476	60	W	19.73
2015 Apr 24 20:17:15.845	60	W	19.53
2015 Apr 24 20:17:15.791	60	W	19.77
2015 Mar 25 20:49:45.774	60	W	19.69
2015 Mar 25 20:49:45.757	60	W	19.77
2015 Mar 25 20:36:26.963	60	W	19.72
2015 Mar 25 20:36:26.946	60	W	19.60
2015 Mar 25 20:25:13.801	60	W	19.61
2015 Mar 25 20:25:13.765	60	W	19.50
2015 Feb 26 22:27:08.995	60	W	19.44
2015 Feb 26 22:27:08.323	60	W	19.47
2015 Feb 26 22:12:35.418	60	W	19.43
2015 Feb 26 22:12:35.357	60	W	19.35
2015 Feb 26 21:51:36.812	60	W	19.43
2015 Feb 26 21:51:36.609	60	W	19.32
2015 Jan 21 00:17:56.9	60	W	19.75
2015 Jan 20 00:18:10.584	60	W	19.73
2015 Jan 20 00:18:10.536	60	W	19.70
2015 Jan 20 00:16:30.601	60	W	19.63
2015 Jan 20 00:16:30.455	60	W	19.64
2015 Jan 20 00:14:52.539	60	W	19.68
2015 Jan 20 00:14:52.539	180	W	20.22
2015 Jan 20 00:14:52.439	60	W	19.60
2015 Jan 20 00:14:52.439	180	W	20.16
2015 Jan 17 00:49:44.307	60	W	19.43
2015 Jan 17 00:49:44.121	60	W	19.30
2015 Jan 17 00:47:41.118	60	W	19.10
2015 Jan 17 00:47:40.16	60	W	18.95
2015 Jan 17 00:45:46.426	180	W	19.90
2015 Jan 17 00:45:46.426	60	W	19.50
2015 Jan 17 00:45:46.291	60	W	19.36
2015 Jan 17 00:45:46.291	180	W	19.73

into account the evolution of star formation for the entire universe (Lipunov et al. 1995).

It was found that NS mergers in a Milky-Way-type galaxy (i.e., in a galaxy with the mass of 10^{11} solar mass and star formation of one solar mass per year) occur at a rate of $\sim 10^{-4}$ yr^{-1} (Lipunov et al. 1987; see the caption to Figure 2, case "e," in that paper). It immediately follows from this that in our neighborhood one merger per year should occur within the sphere containing 10,000 galaxies of the Milky Way type. This volume corresponds to the radius of $D \sim 20$ Mpc . Hence, the first Monte Carlo population synthesis in 1987 predicted an occurrence rate of several events per year within the sphere of radius ~ 40 Mpc, which agreed with 2017 observations quite well. Note that the work of Phinney (1991), using estimations from pulsar binary period deviation, gave a rate of two orders lower for merging NSs.

The proximity of GW170817 is entirely consistent with the evolution of NS–NS merger rates in the universe later computed using the Scenario Machine (Lipunov et al. 1995; Lipunov & Pruzhinskaya 2014, cf. Belczynski et al. 2002).

Even if the line of sight to a GRB is not co-aligned with the jet during the merger (the corresponding probability is close to 99.9%), the event may still produce more isotropic accompanying, or even leading, radiation.

The possibility of a kilonova explosion resulting from the decay of radioactive elements in the expanding envelope was discussed in Li & Paczynski (1998), Freiburghaus et al. (1999), Rosswog et al. (1999), Rosswog (2005), Metzger et al. (2010), and Coughlin et al. (2017).

A number of very important arguments supporting the hypothesis that SSS17a is a kilonova candidate were published based on the analysis of the wideband photometry (see Abbott et al. 2017b) and spectral observations (Abbott et al. 2017b; Drout et al. 2017; Shara et al. 2017) .

Let us now compare the observed optical luminosity with the optical luminosities of other possible kilonovae observed earlier, namely for GRB 130603B (Tanvir et al. 2013) and GRB 080503 (Perley et al. 2009; see Table 2). For the maximum brightness of the kilonova in NGC 4993, we use the first point on the MASTER light curve (Figure 3). We use the redshifts for the two galaxies that are visually closest to the GRB position (see the discussion below).

The source spectra are unknown and, following Perley et al. (2009, Figure 7), we use a flat spectrum to estimate the k correction. Hence, $M = m$–DM$+2.5 \log(1+z)$, where DM is the distance modulus. Furthermore, for flat-spectrum sources the absolute magnitudes in all bins are equal.

We assume that the redshift of GRB 080503 is equal to the redshifts of the two galaxies visually closest to it. However, there remains no consensus regarding the host galaxy of GRB 080503. Perley et al. (2009) suggested that the nearest galaxies have no connection with GRB 080503 due to large angular separations. However, we believe that any of these galaxies could potentially be a host because NS–NS systems must obtain a huge kick velocity during the two SN explosions, allowing them to escape from the galaxy before the collision. In any case, this is the unique and best estimate of the redshift for a given object.

The agreement between the observed absolute magnitudes and characteristic luminosities evoke the old idea about viewing GRBs as standard candles (Lipunov et al. 2001). However, we are now dealing with kilonovae that accompany short GRB events. Here we have rather an analogy with Type Ia supernovae (SNe). Both kinds of event may represent collisions of compact stars: binary white dwarfs and binary NSs in the case of supernovae and kilonovae, respectively. In addition, the mass of the collapsing object may also play an important part in both processes: the Chandrasekhar limit for SN Ia, and the Oppenheimer—Volkov limit for kilonovae. Of course this reasoning may be too naive, given that the densities of objects differ by a million fold. Also, a kilonova is fainter than an SN Ia and does not have simple spectral lines. Due to the kick velocity, double NS systems can escape from their host galaxies. In this case, the brightness of the kilonova is only one indicator of its distance.

Furthermore, optical radiation plays an important part in the energy balance of SN Ia, whereas this is by no means evident in the case of kilonovae, for which the total energy release in the infrared and X-ray parts of the spectrum can be more important. In this connection, of interest is the discovery of X-ray emission from kilonova in NGC 4993 (Troja et al. 2017), which provides new information about the astrophysical properties of the kilonova.

ORCID iDs

V. M. Lipunov https://orcid.org/0000-0003-3668-1314
R. Rebolo https://orcid.org/0000-0003-3767-7085
M. Serra-Ricart https://orcid.org/0000-0002-2394-0711
Xiaofeng Wang https://orcid.org/0000-0002-7334-2357

References

Abbott, B. P., Abbott, R., Abbott, T. D., et al. 2016a, ApJ, 818L, 22
Abbott, B. P., Abbott, R., Abbott, T. D., et al. 2016b, PhRvL, 116, 061102
Abbott, B. P., Abbott, R., Abbott, T. D., et al. 2016c, ApJL, 826, 13
Abbott, B. P., Abbott, R., Abbott, T. D., et al. 2017a, PhRvL, 119, 161101
Abbott, B. P., Abbott, R., Abbott, T. D., et al. 2017b, ApJL, 848, L12
Alard, C. 2000, A&AS, 144, 363
Bartos, I., Countryman, S., Finley, C., et al. 2017, GCN, 21508, https://gcn.gsfc.nasa.gov/gcn3/21508.gcn3
Belczynski, K., Kalogera, V., & Bulik, T. 2002, ApJ, 572, 407
Berger, E., Fong, W., & Chornock, R. 2013, ApJ, 774L, 23
Blinnikov, S. I., Novikov, I. D., Perevodchikova, T. V., & Polnarev, A. G. 1984, SvAL, 10, 177
Chambers, K. C., Huber, M. E., Smartt, S. J., et al. 2017, GCN, 21553, https://gcn.gsfc.nasa.gov/gcn3/21553.gcn3
Chen, T.-W., Wiseman, P., Greiner, J., et al. 2017, GCN, 21592, https://gcn.gsfc.nasa.gov/gcn3/21592.gcn3
Clark, J. P. A., van den Heuvel, E. P. J., & Sutantyo, W. 1979, A&A, 72, 120
Connaughton, V., Blackburn, L., Briggs, M. S., et al. 2017, GCN, 21506, https://gcn.gsfc.nasa.gov/gcn3/21506.gcn3
Cook, D. O., Van Sistine, A., Singer, L., & Kasliwal, M. M. 2017, GCN, 21519, https://gcn.gsfc.nasa.gov/gcn3/21519.gcn3
Coughlin, M., Dietrich, T., Kawaguchi, K., et al. 2017, ApJ, 849, 12
Coulter, C. D., Kilpatrick, M. R., & Siebert 2017, GCN, 21529, https://gcn.gsfc.nasa.gov/gcn3/21529.gcn3
Drout, J. D., Simon, B. J., Shappee, B. J., et al. 2017, GCN, 21547, https://gcn.gsfc.nasa.gov/gcn3/21547.gcn3
Freiburghaus, C., Rosswog, S., & Thielemann, F.-K. 1999, ApJL, 525, L121

Gorbvskoy, E., Ivanov, K., Lipunov, V., et al. 2010, AdAst, 2010, 62
Gorbovskoy, E., Lipunov, V., Kornilov, V., et al. 2013, ARep, 57, 233
Hansen, B. M. S., & Lyutikov, M. 2001, MNRAS, 322, 695
Kornilov, V., Lipunov, V., Gorbovskoy, E., et al. 2012, ExA, 33, 173
Li, L.-X., & Paczynski, B. 1998, ApJL, 507, L59
LIGO Scientific Collaboration & Virgo Collaboration 2017a, GCN, 21505, https://gcn.gsfc.nasa.gov/gcn3/21505.gcn3
LIGO Scientific Collaboration & Virgo Collaboration 2017b, GCN, 21509, https://gcn.gsfc.nasa.gov/gcn3/21509.gcn3
LIGO Scientific Collaboration & Virgo Collaboration 2017c, GCN, 21513, https://gcn.gsfc.nasa.gov/gcn3/21513.gcn3
Lipunov, V. 2017, GCN, 21621, https://gcn.gsfc.nasa.gov/gcn3/21621.gcn3
Lipunov, V., Gorbovskoy, E., Kornilov, V., et al. 2017a, GCN, 21546, https://gcn.gsfc.nasa.gov/gcn3/21546.gcn3
Lipunov, V., Gorbovskoy, E., Kornilov, V., et al. 2017b, GCN, 21570, https://gcn.gsfc.nasa.gov/gcn3/21570.gcn3
Lipunov, V., Gorbovskoy, E., Kornilov, V., et al. 2017c, GCN, 21587, https://gcn.gsfc.nasa.gov/gcn3/21587.gcn3
Lipunov, V., Gorbovskoy, E., Kornilov, V., et al. 2017d, GCN, 21687, https://gcn.gsfc.nasa.gov/gcn3/21687.gcn3
Lipunov, V., Kornilov, V., Gorbovkoy, E., et al. 2010, AdAst, 2010, 30
Lipunov, V., Postnov, K. A., Prokhorov, M. E., Panchenko, I. E., & Jorgensen, H. E. 1995, ApJ, 454, 593
Lipunov, V., & Pruzhinskaya, M. 2014, MNRAS, 440, 1193
Lipunov, V. M., & Gorbovskoy, E. S. 2008, MNRAS, 383, 1397
Lipunov, V. M., Gorosabel, J., Pruzhinskaya, M., et al. 2016, MNRAS, 455, 712
Lipunov, V. M., Kornilov, V., Gorbovskoy, E., et al. 2017e, MNRAS, 465, 3656
Lipunov, V. M., Kornilov, V., Gorbovskoy, E., et al. 2017f, NewA, 51, 122
Lipunov, V. M., & Panchenko, I. E. 1996, A&A, 312, 937
Lipunov, V. M., Postnov, K. A., & Prokhorov, M. E. 1987, A&A, 176, L1
Lipunov, V. M., Postnov, K. A., & Prokhorov, M. E. 2001, ARep, 45, 236
Lipunova, G. V., Gorbovskoy, E. S., Bogomazov, A. I., & Lipunov, V. M. 2009, MNRAS, 397, 1695
Lipunova, G. V., & Lipunov, V. M. 1998, A&A, 329, L29
Metzger, B. D., Martínez-Pinedo, G., & Darbha, S. 2010, MNRAS, 406, 2650
Perley, D. A., Metzger, B. D., Granot, J., et al. 2009, ApJ, 696, 1871
Phinney, E. S. 1991, ApJL, 380, L17
Pian, E., D'Elia, V., Piranomonte, S., et al. GCN, 21592, https://gcn.gsfc.nasa.gov/gcn3/21592.gcn3
Rosswog, S. 2005, AJ, 634, 1202
Rosswog, S., Liebendörfer, M., Thielemann, F.-K., et al. 1999, A&A, 341, 499
Savchenko, V., Mereghetti, S., & Ferrigno, C. 2017, GCN, 21513, https://gcn.gsfc.nasa.gov/gcn3/21513.gcn3
Schlafly, E. F., & Finkbeiner, D. P. 2011, ApJ, 737, 103
Shara, T., Williams, P., Vaisanen, P., et al. 2017, GCN, 21610, https://gcn.gsfc.nasa.gov/gcn3/21610.gcn3
Singer, L. P., Chen, H.-Yu., Holz, D. E., et al. 2016, ApJL, 829, L15
Singer, L. P., & Price, L. R. 2016, PhRvD, 93, 024013
Tanvir, N. R., Levan, A. J., Fruchter, A. S., et al. 2013, Natur, 500, 547
Troja, E., Lipunov, V., Mundel, C., et al. 2017a, Natur, 547, 425
Troja, E., Piro, L., Sakamoto, T., et al. 2017b, GCN, 21765, https://gcn.gsfc.nasa.gov/gcn3/21765.gcn3
von Kienlin, A., Meegan, C., & Goldstein, A. 2017, GCN, 21520, https://gcn.gsfc.nasa.gov/gcn3/21520.gcn3
Yurkov, V., Sergienko, Yu., Varda, D., et al. 2016, GCN, 20063